Supporting Information (SI)

Novel Iron(III)-Based Metal-Organic Gels with Superior Catalytic Performance Towards Luminol Chemiluminescence

Li He, [†] *Zhe Wei Peng,* [†] *Zhong Wei Jiang,* [‡] *Xue Qian Tang,* [†] *Cheng Zhi Huang,** [‡] *and Yuan Fang Li** [†]

[†]Key Laboratory of Luminescent and Real-Time Analytical Chemistry (Southwest University), Ministry of Education, College of Chemistry and Chemical Engineering, Southwest University, Chongqing 400715, China. E-mail: liyf@swu.edu.cn,
Tel: (+86) 23 68254659, Fax: (+86) 23 68367257.
[‡] College of Pharmaceutical Sciences, Southwest University, Chongqing 400716, China.
E-mail: chengzhi@swu.edu.cn.

Supporting figures

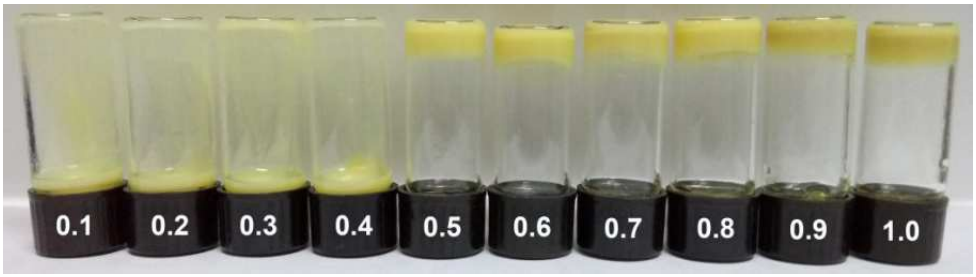

Figure S1. Snapshots of inverted vials of Fe-MOGs. Numbers on the cap indicate the equivalents of metal salt with respect to PDA present in the respective vial.

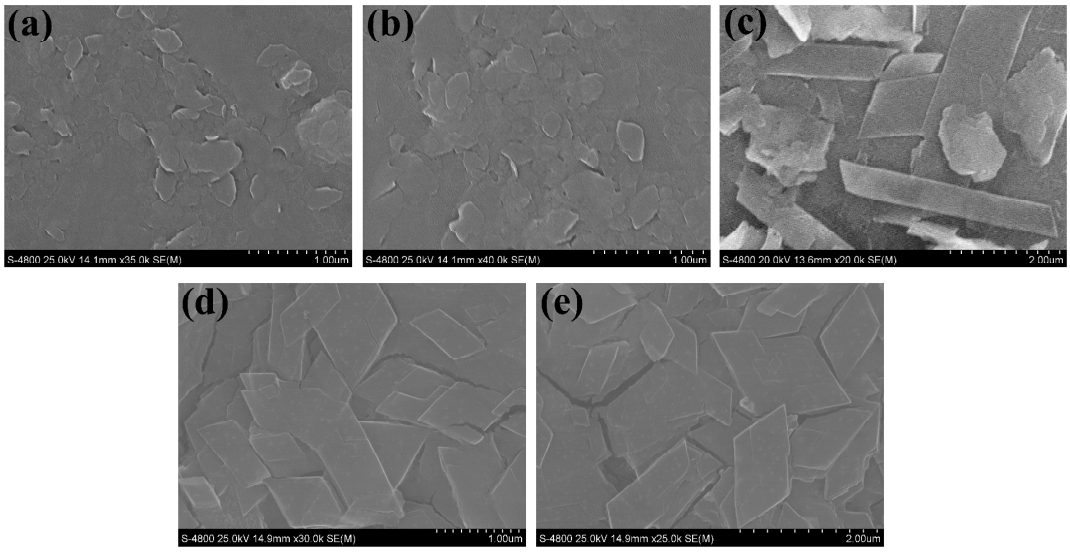

Figure S2. SEM images of Fe-MOXs over a wide pH range: (a) pH 2.84, (b) pH 4.07, (c) pH 6.47, (d) pH 8.02, (e) pH 9.86.

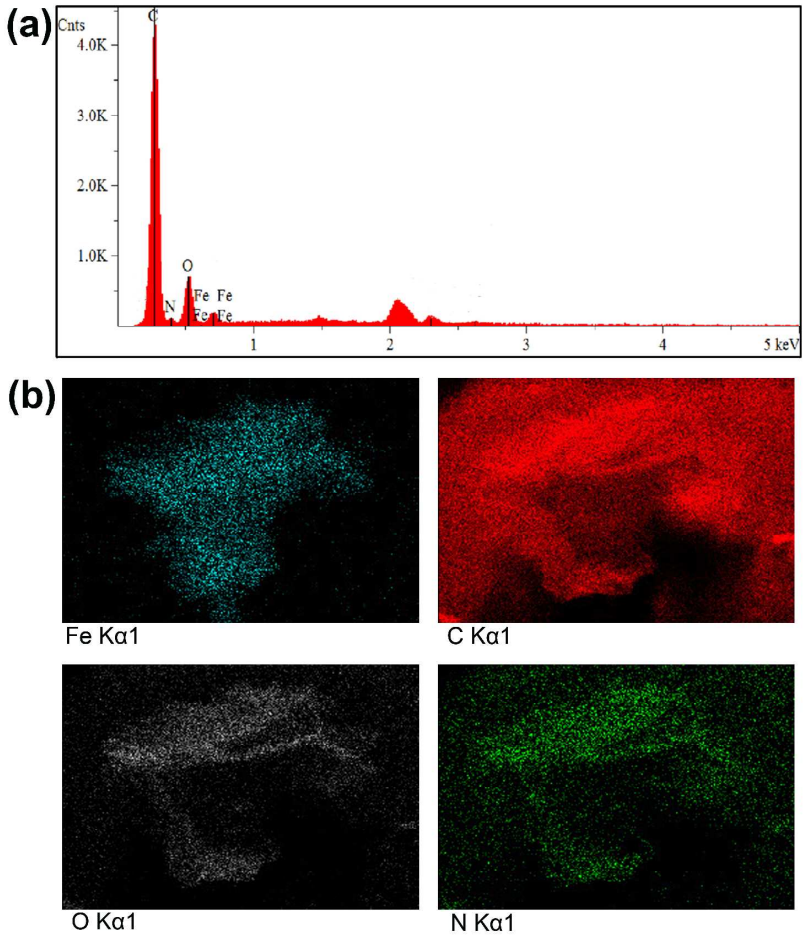

Figure S3. (a) EDAX pattern and (b) elemental-mapping analysis of Fe-MOXs showing the presence of Fe, C, O and N as the constitutional elements.

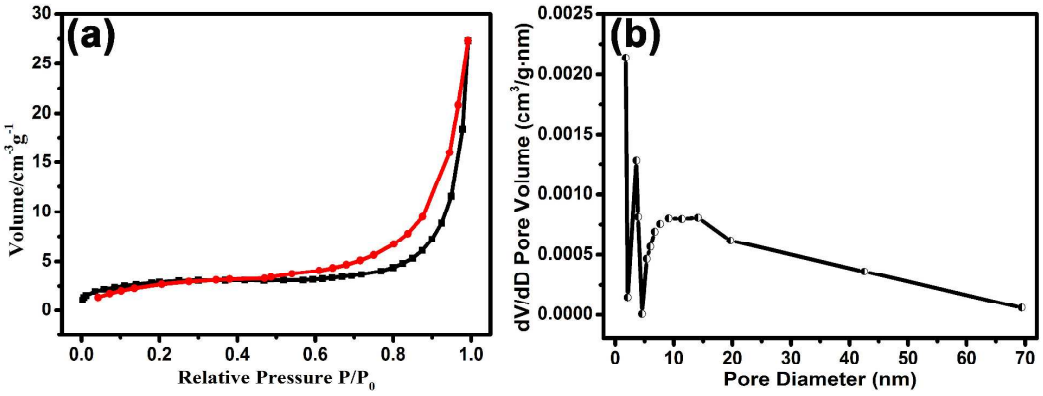

Figure S4. (a) N_2 gas adsorption-desorption isotherm and (b) pore size distribution profiles of Fe-MOXs. (Total surface area, 10.17 m^2g^{-1}; total pore volume, 0.042 cm^3g^{-1}; N_2 gas uptake capacity,

27.28 cm^3g^{-1}.)

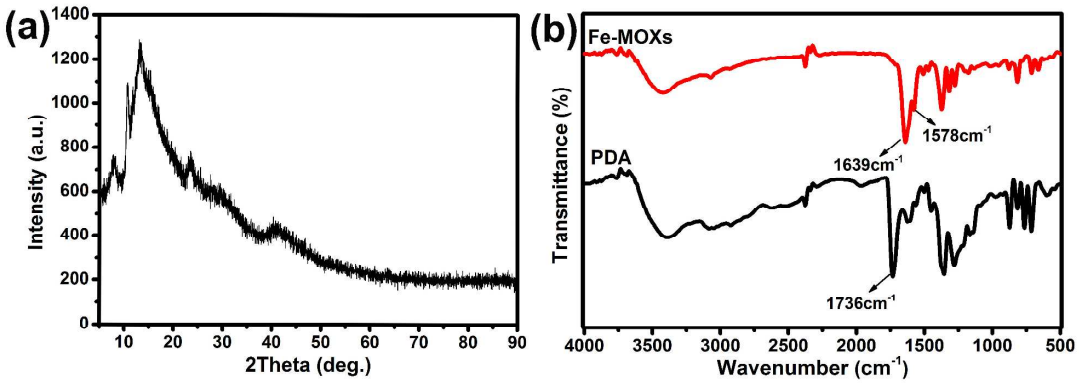

Figure S5. (a) X-ray powder diffraction patterns of Fe-MOXs and (b) FT-IR spectra of PDA and Fe-MOXs.

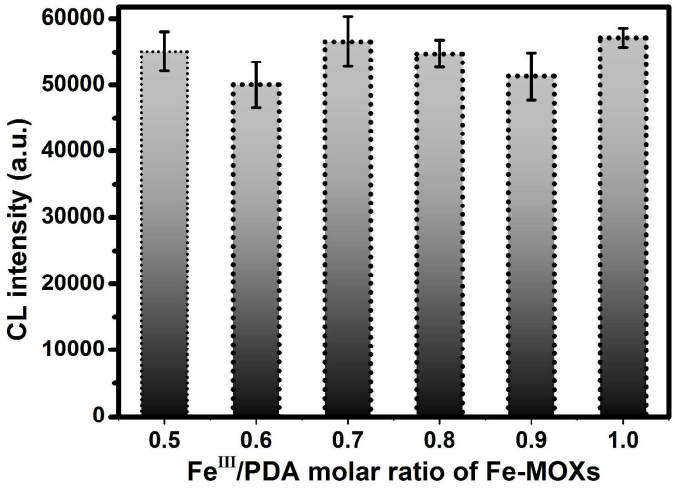

Figure S6. The contrast experiments of the catalytic ability of Fe-MOXs at the molar raitio of Fe^{III}/PDA from 0.5 to 1.0. Experimental conditions: Fe-MOXs, 0.1 mg/mL; luminol, 0.7 mM in 0.2 M BR buffer solution (pH 9.27).

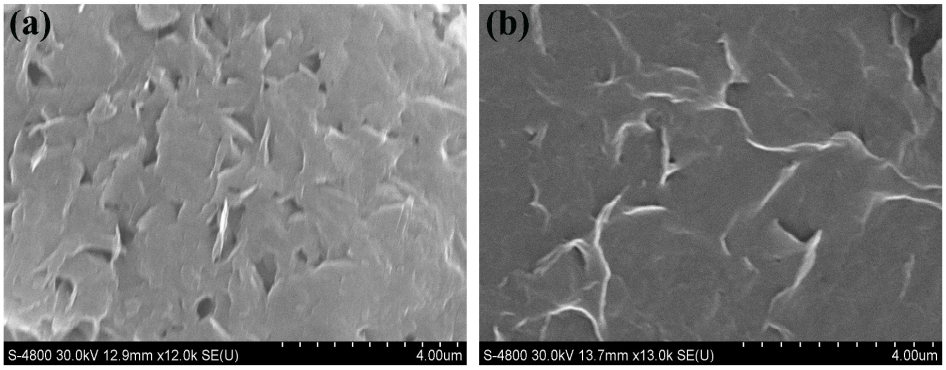

Figure S7. The SEM images of Fe-MOXs (a) before and (b) after CL reaction.

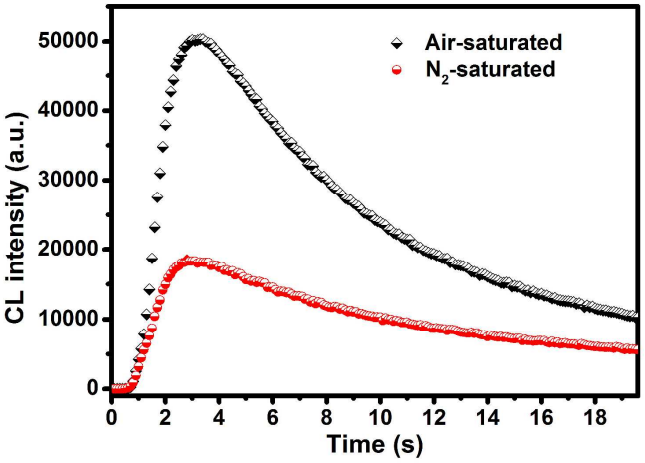

Figure S8. CL response curves of luminol-Fe-MOXs system under air-saturated (black line) and nitrogen-saturated solution (red line), respectively. The nitrogen-saturated reactant solution was bubbled with N_2 for 1 h (red), while the air-saturated solution was not bubbled (black).

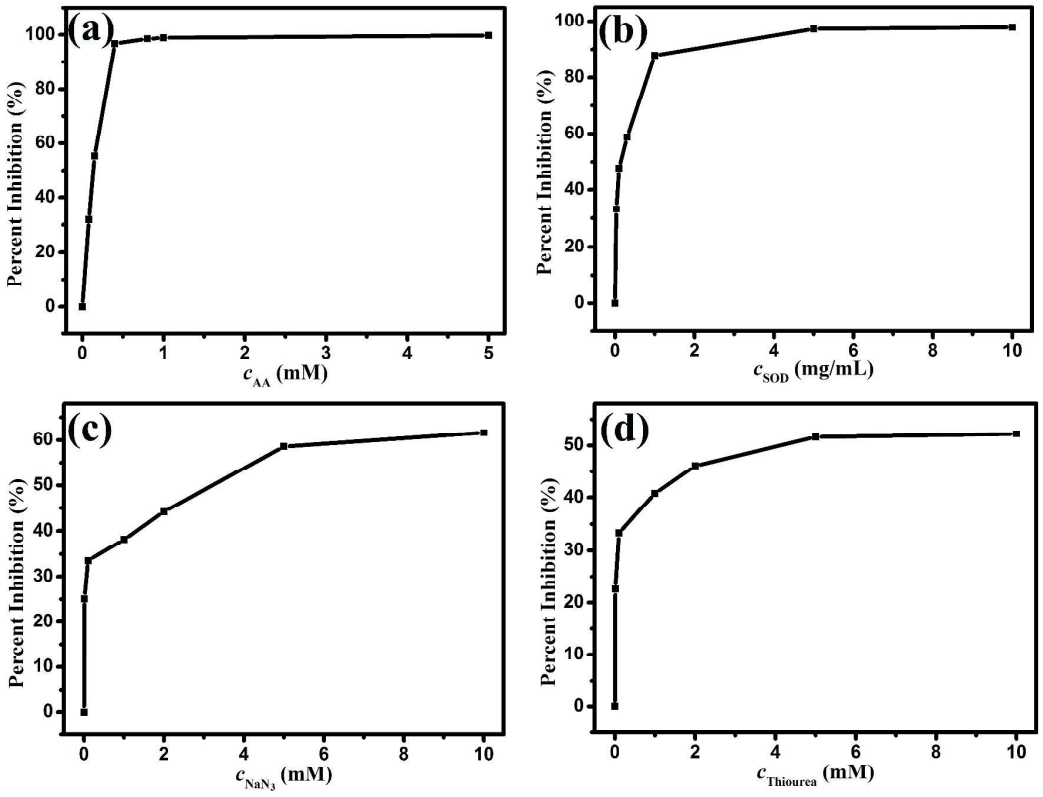

Figure S9. Effects of the radical scavengers of (a) AA, (b) SOD, (c) NaN_3, and (d) thiourea on the luminol-Fe-MOXs CL system. Final concentrations: Fe-MOXs, 0.1 mg/mL; luminol, 0.7 mM in BR buffer solution (pH 9.27).

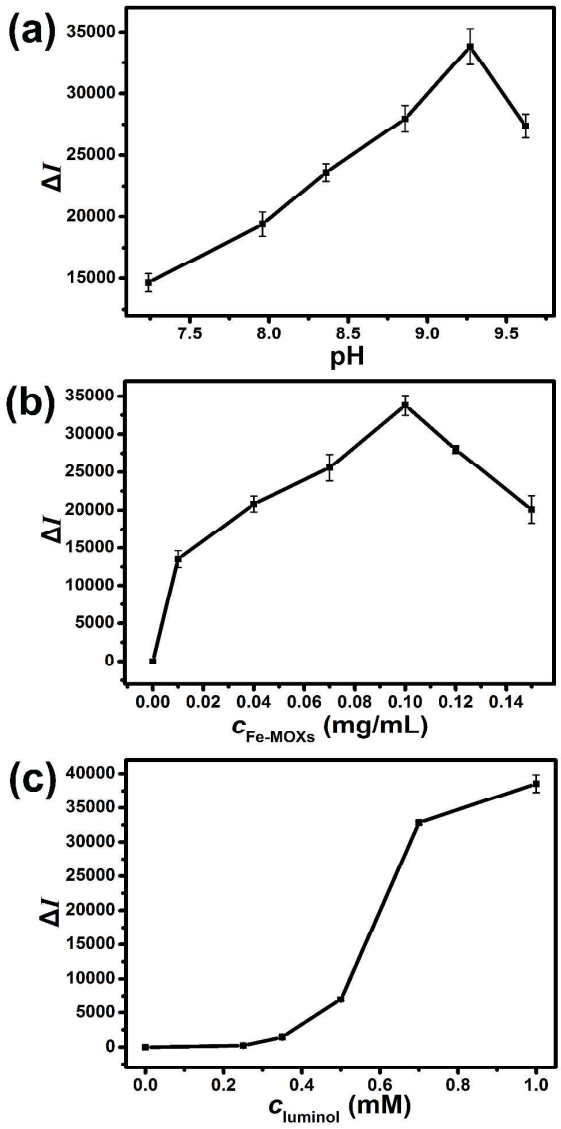

Figure S10. Effects of the reactant conditions on luminol CL system in the presence of Fe-MOXs. (a) Effect of luminol pH: 0.7 M luminol, 0.1 mg/mL Fe-MOXs. (b) Effect of Fe-MOXs concentration: 0.7 M luminol in BR buffer solution (pH 9.27). (c) Effect of luminol concentration: BR buffer solution (pH 9.27), 0.1 mg/mL Fe-MOXs.

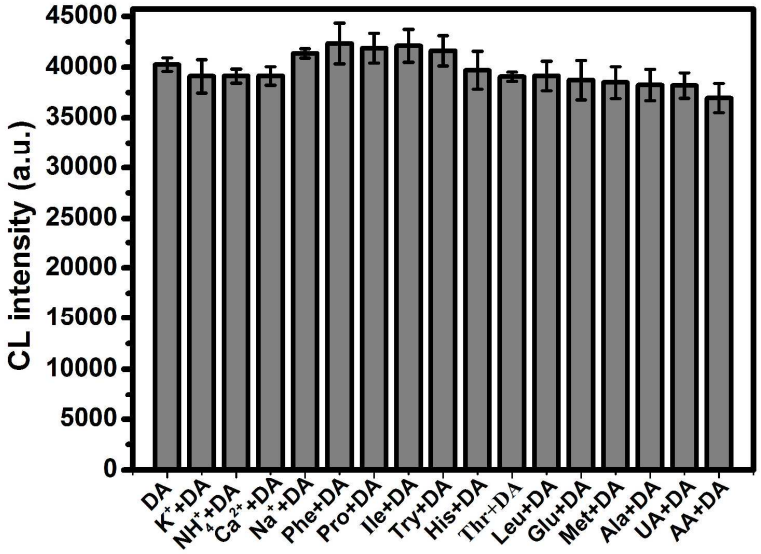

Figure S11. Investigation on the interfering effects of other co-existing substances for the detection of DA. The ratios of co-existing chemical components tolerated in analysis of DA (0.1μM) were 1000-fold for K^+, NH_4^+, Ca^{2+} and Na^+, 50-fold for phenylalanine (Phe), proline (Pro), Isoleucine (Ile), tryptophan (Try), histidine (His), threonine (Thr), leucine (Leu), glutamic acid (Glu), methionine (Met), alanine (Ala), and 5-fold for uric acid (UA), ascorbic acid (AA).

Table S1. A comparison of different analytical techniques for the determination of dopamine.

Detection method	*Materials*	*LOD(nM)*	*Linear range(μM)*	*Ref.*
Fluorescence	F-$CuInS_2$ QDs	200	0.5-40	1
Colorimetry	AHMT-AuNPs	70	0.2-1.1	2
Colorimetry	AgNPs	60	0-0.6	3
Electrochemical	Graphene/SnO_2 modified electrode	80	0.1-10	4
Electrochemiluminescence	CdSeTe/ZnS core-shell quantum dots	100	0.375-450	5
Electrochemiluminescence	$K_2S_2O_8$-Ag_2SeQD	100	0.500-19	6
Electrochemiluminescence	CdSe QDs	500	0.5-70	7
Electrochemiluminescence	MPA-modified CdTe QDs	50	0.05-5.0	8
Electrochemiluminescence	CdSe/ZnS QD	50	0.1-20	9
Chemiluminescence	Fe-MOXs	20.4	0.05-0.6	This work

REFERENCES

(1) Anithaa, A. C.; Lavanya, N.; Asokan, K.; Sekar, C. WO_3 Nanoparticles Based Direct Electrochemical Dopamine Sensor in the Presence of Ascorbic Acid. *Electrochim. Acta* **2015,** *167*, 294－302.

(2) Feng, J. J.; Guo, H.; Li, Y. F.; Wang, Y. H.; Chen, W. Y.; Wang, A. J. Single Molecular Functionalized Gold Nanoparticles for Hydrogen-Bonding Recognition and Colorimetric Detection of Dopamine with High Sensitivity and Selectivity. *ACS Appl. Mater. Interfaces* **2013,** *5*, *1226－1231*.

(3) Lin, Y. H.; Chen, C. E.; Wang, C. Y.; Pu, F.; Ren, J. S.; Qu, X. G. Silver Nanoprobe for Sensitive and Selective Colorimetric Detection of Dopamine via Robust Ag-Catechol Interaction. *Chem. Commun.* **2011,** *47*, *1181－1183*.

(4) Yang, A. K.; Xue, Y.; Zhang, Y.; Zhang, X. F.; Zhao, H.; Li, X. J.; He, Y. J.; Yuan, Z. B. A Simple One-Pot Synthesis of Graphene Nanosheet/SnO2 Nanoparticle Hybrid Nanocomposites and Their Application for Selective and Sensitive Electrochemical Detection of Dopamine. *J. Phys. Chem. B* **2013,** *1*, 1804－1811.

(5) Stewart, A. J.; Hendry, J.; Dennany, L. Whole Blood Electrochemiluminescent Detection of Dopamine. *Anal. Chem.* **2015,** *87*, 11847－11853.

(6) Cui, R.; Gu, Y. P.; Bao, L.; Zhao, J. Y.; Qi, B. P.; Zhang, Z. L.; Xie, Z. X.; Pang, D. W. Near-Infrared Electrogenerated Chemiluminescence of Ultrasmall Ag_2Se Quantum Dots for the Detection of Dopamine. *Anal. Chem.* **2012,** *84*, 8932－89355.

(7) Liu, X.; Cheng, L. X.; Lei, J. P.; Ju, H. X. Dopamine Detection Based on its Quenching Effect on the Anodic Electrochemiluminescence of CdSe Quantum Dots. *Analyst* **2008,** *133*, 1161－1163.

(8) Liu, X.; Jiang, H.; Lei, J. P.; Ju, H. X. Anodic Electrochemiluminescence of CdTe Quantum Dots and Its Energy Transfer for Detection of Catechol Derivatives. *Anal. Chem.* **2007,** *79*, 8055－8060.

(9) Bao, L.; Sun, L. F.; Zhang, Z. L.; Jiang, P.; Wise, F. W.; Abruña, H. c. D.; Pang, D. W. Energy-Level-Related Response of Cathodic Electrogenerated-Chemiluminescence of Self-Assembled CdSe/ZnS Quantum Dot Films. *J. Phys. Chem. C* **2011,** *115*, 18822－18828.